# Polarization-insensitive fiber-coupled superconducting-nanowire single photon detector using a high-index dielectric capping layer

ANNA MUKHTAROVA,[1] LUCA REDAELLI,[1] DIBYENDU HAZRA,[1] HOUSSAINE MACHHADANI,[1] STÉPHANE LEQUIEN,[2] MAX HOFHEINZ,[1] JEAN-LUC THOMASSIN,[1] FREDERIC GUSTAVO,[1] JULIEN ZICHI,[3] VAL ZWILLER,[1,3,4] EVA MONROY,[1,*] AND JEAN-MICHEL GÉRARD[1]

[1]*Univ. Grenoble Alpes, CEA, INAC, PHELIQS, 17 av. des Martyrs, F38000, Grenoble, France*
[2]*Univ. Grenoble Alpes, CEA, INAC, MEM, 17 av. des Martyrs, F38000, Grenoble, France*
[3]*KTH Stockholm, Department of Applied Physics, SE-114, 128 Stockholm, Sweden*
[4]*TU Delft, Kavli Institute of Nanoscience, Lorentzweig 1, 2628 CJ Delft, the Netherlands*
*[*]eva.monroy@cea.fr*

**Abstract:** Superconducting-nanowire single photon detectors (SNSPDs) are able to reach near-unity detection efficiency in the infrared spectral range. However, due to the intrinsic asymmetry of nanowires, SNSPDs are usually very sensitive to the polarization of the incident radiation, their responsivity being maximum for light polarized parallel to the nanowire length (transverse-electric (TE) polarization). Here, we report on the reduction of the polarization sensitivity obtained by capping NbN-based SNSPDs with a high-index SiNx dielectric layer, which reduces the permittivity mismatch between the NbN wire and the surrounding area. Experimentally, a polarization sensitivity below 0.1 is obtained both at 1.31 and 1.55 μm, in excellent agreement with simulations.

## References and links

1. C. M. Natarajan, M. G. Tanner, and R. H. Hadfield, "Superconducting nanowire single-photon detectors: physics and applications," Supercond. Sci. Technol. **25**(6), 063001 (2012).
2. E. A. Dauler, M. E. Grein, A. J. Kerman, F. Marsili, S. Miki, S. W. Nam, M. D. Shaw, H. Terai, V. B. Verma, and T. Yamashita, "Review of superconducting nanowire single-photon detector system design options and demonstrated performance," Opt. Eng. **53**(8), 081907 (2014).
3. S. Miki, T. Yamashita, M. Fujiwara, M. Sasaki, and Z. Wang, "Multichannel SNSPD system with high detection efficiency at telecommunication wavelength," Opt. Lett. **35**(13), 2133–2135 (2010).
4. M. G. Tanner, C. M. Natarajan, V. K. Pottapenjara, J. A. O'Connor, R. J. Warburton, R. H. Hadfield, B. Baek, S. Nam, S. N. Dorenbos, E. B. Ureña, T. Zijlstra, T. M. Klapwijk, and V. Zwiller, "Enhanced telecom wavelength single-photon detection with NbTiN superconducting nanowires on oxidized silicon," Appl. Phys. Lett. **96**(22), 221109 (2010).
5. L. Redaelli, G. Bulgarini, S. Dobrovolskiy, S. N. Dorenbos, V. Zwiller, E. Monroy, and J. M. Gérard, "Design of broadband high-efficiency superconducting-nanowire single photon detectors," Supercond. Sci. Technol. **29**(6), 065016 (2016).
6. F. Marsili, V. B. Verma, J. A. Stern, S. Harrington, A. E. Lita, T. Gerrits, I. Vayshenker, B. Baek, M. D. Shaw, R. P. Mirin, and S. W. Nam, "Detecting single infrared photons with 93% system efficiency," Nat. Photonics **7**(3), 210–214 (2013).
7. I. Esmaeil Zadeh, J. W. N. Los, R. B. M. Gourgues, V. Steinmetz, G. Bulgarini, S. M. Dobrovolskiy, V. Zwiller, and S. N. Dorenbos, "Single-photon detectors combining high efficiency, high detection rates, and ultra-high timing resolution," APL Photonics **2**(11), 111301 (2017).
8. L. Redaelli, V. Zwiller, E. Monroy, and J. M. Gérard, "Design of polarization-insensitive superconducting single photon detectors with high-index dielectrics," Supercond. Sci. Technol. **30**(3), 035005 (2017).
9. V. Anant, A. J. Kerman, E. A. Dauler, J. K. W. Yang, K. M. Rosfjord, and K. K. Berggren, "Optical properties of superconducting nanowire single-photon detectors," Opt. Express **16**(14), 10750–10761 (2008).

10. S. N. Dorenbos, E. M. Reiger, N. Akopian, U. Perinetti, V. Zwiller, T. Zijlstra, and T. M. Klapwijk, "Superconducting single photon detectors with minimized polarization dependence," Appl. Phys. Lett. **93**(16), 161102 (2008).
11. J. Huang, W. J. Zhang, L. X. You, X. Y. Liu, Q. Guo, Y. Wang, L. Zhang, X. Y. Yang, H. Li, Z. Wang, and X. M. Xie, "Spiral superconducting nanowire single-photon detector with efficiency over 50% at 1550 nm wavelength," Supercond. Sci. Technol. **30**(7), 074004 (2017).
12. C. Gu, Y. Cheng, X. Zhu, and X. Hu, "Fractal-Inspired, Polarization-Insensitive Superconducting Nanowire Single-Photon Detectors," OSA Tech. Dig. Online JM3A.10 (2015).
13. V. B. Verma, F. Marsili, S. Harrington, A. E. Lita, R. P. Mirin, and S. W. Nam, "A three-dimensional, polarization-insensitive superconducting nanowire avalanche photodetector," Appl. Phys. Lett. **101**(25), 251114 (2012).
14. V. B. Verma, B. Korzh, F. Bussières, R. D. Horansky, S. D. Dyer, A. E. Lita, I. Vayshenker, F. Marsili, M. D. Shaw, H. Zbinden, R. P. Mirin, and S. W. Nam, "High-efficiency superconducting nanowire single-photon detectors fabricated from MoSi thin-films," Opt. Express **23**(26), 33792–33801 (2015).
15. F. Zheng, R. Xu, G. Zhu, B. Jin, L. Kang, W. Xu, J. Chen, and P. Wu, "Design of a polarization-insensitive superconducting nanowire single photon detector with high detection efficiency," Sci. Rep. **6**(1), 22710 (2016).
16. R. Xu, F. Zheng, D. Qin, X. Yan, G. Zhu, L. Kang, L. Zhang, X. Jia, X. Tu, B. Jin, W. Xu, J. Chen, and P. Wu, "Demonstration of Polarization-Insensitive Superconducting Nanowire Single-Photon Detector With Si Compensation Layer," J. Lightwave Technol. **35**(21), 4707–4713 (2017).
17. M. Björck and G. Andersson, "*GenX*: an extensible X-ray reflectivity refinement program utilizing differential evolution," J. Appl. Cryst. **40**(6), 1174–1178 (2007).
18. A. Semenov, B. Günther, U. Böttger, H.-W. Hübers, H. Bartolf, A. Engel, A. Schilling, K. Ilin, M. Siegel, R. Schneider, D. Gerthsen, and N. A. Gippius, "Optical and transport properties of ultrathin NbN films and nanostructures," Phys. Rev. B **80**(5), 054510 (2009).
19. A. J. Miller, A. E. Lita, B. Calkins, I. Vayshenker, S. M. Gruber, and S. W. Nam, "Compact cryogenic self-aligning fiber-to-detector coupling with losses below one percent," Opt. Express **19**(10), 9102–9110 (2011).

## 1. Introduction

The demand for reliable and efficient single photon detectors has significantly increased during the last years, driven by emerging applications in the domains of quantum cryptography, space-to-ground communication, integrated circuit testing, etc. Single-photon detectors based on superconducting nanowires (SNSPD) are a promising technology for operation at telecommunication wavelengths [1–5]. Detection efficiency around 90% has been demonstrated for microcavity-based devices working under normal incidence illumination [6,7]. However, the response of SNSPDs is strongly dependent on the polarization of the incoming light due to the meandering nanowire geometry. The efficiency is maximum for transverse-electric (TE) polarization, where the electric field oscillates along the nanowire length, and drops down for transverse-magnetic (TM) polarized light, where the electric field oscillates along the nanowire width [5,8,9]. Several solutions have been proposed to overcome this problem. It was first suggested to replace the nanowire meander by a helical structure, which allows a significant reduction of the polarization sensitivity, but at the same time averages the overall detection efficiency for both polarizations [10,11]. Fractal patterning of the nanowires has also been proposed as an alternative approach [12]. On the other hand, Verma *et al.* showed that polarization-insensitive devices with high detection efficiency can be achieved by stacking and electrically connecting two SNSPDs with orthogonal meanders [13]. However, the fabrication of such a device is particularly challenging since the second nanowire must be deposited and patterned on top of a non-uniform surface. A reduction of the polarization sensitivity has been observed when using amorphous silicides (WSi, MoSi) as superconducting material capped with $SiO_2$ [6,14]. However, this comes at the price of a significantly lower superconducting critical temperature (below 4 K for WSi and MoSi, to be compared to 8-10 K for thin films of NbN or NbTiN).

It is also possible to erase polarization sensitivity without modification of the meander geometry by reducing the permittivity mismatch between the nanowire and its surroundings. Thus, Zheng *et al.* have designed polarization-insensitive devices for which a high permittivity material such as silicon is wrapped around the superconducting nanowire [15]. Simulations showed that it is possible to obtain an absorption efficiency of 96% at 1.55 µm with only 0.5% difference between TE and TM polarizations by inserting such Si-wrapped

nanowires into an optical cavity. Redaelli *et al.* have introduced a more flexible approach, for which only one side of the nanowire (top or bottom) is in contact with a high-index dielectric material such as $Si_3N_4$, $TiO_2$, or semiconductors such as GaAs or Si [8]. Following this approach, reduced polarization sensitivity has been reported for an SNSPD using amorphous silicon as permittivity-matching cap layer [16]. The device incorporates a gold mirror on top of the amorphous silicon, to enhance the response. Therefore, light is applied through the back side of the detector, passing through the silicon substrate. This back-illuminated geometry induces a severe limitation on the device response due to coupling and transmission losses (the device is characterized using a technique of far-field alignment, with coupling efficiency estimated at $2.9 \times 10^{-5}$). Furthermore, the layer sequence, including a silicon substrate on one side and an amorphous silicon layer on the other side, prevents the application of this design for detectors operating at wavelengths below 1.1 µm.

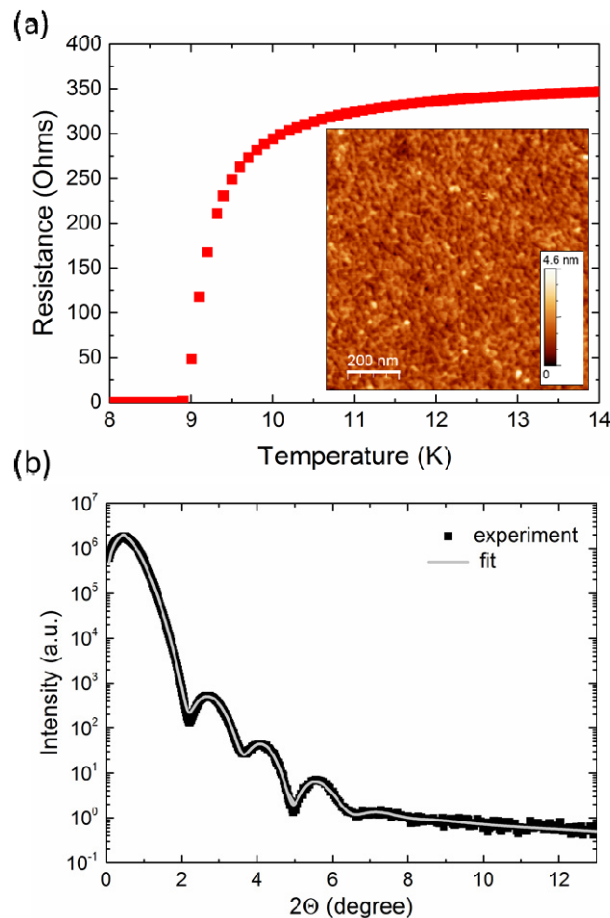

Fig. 1. (a) Film resistance vs. temperature for the NbN thin film under study. Inset: $1 \times 1$ µm2 atomic force microscopy image of the NbN surface. (b) X-ray reflectivity of the NbN film on SiO2-on-silicon. Black squares are experimental measurements and the solid gray line is a fit generated with the GenX software.

In this paper, we present fiber-coupled polarization-insensitive SNSPDs incorporating a $SiN_x$ permittivity-matching cap layer. Such photodetectors are operated under front-side illumination, which simplifies the fabrication process and minimizes the coupling losses. The devices are designed in view of efficient operation over a broad spectral window, including the 1.31 µm and 1.55 µm telecom bands. They are fabricated on a quarter-wavelength $SiO_2$

layer on top of a Si substrate. For an optimized thickness of the $SiN_x$ cap, we demonstrate a strong reduction of the polarization sensitivity, without compromising the detector efficiency for TE polarization. This improvement is due to the decrease of the permittivity mismatch between the nanowire and the surrounding area, which leads to an enhancement of the electric field inside the nanowire, and hence of the absorption coefficient for TM-polarized light.

## 2. Characterization of the superconductor

For the fabrication of the SNSPDs, an NbN film with a nominal thickness of 5 nm was deposited by direct-current magnetron sputtering on a Si substrate covered with a 270-nm-thick thermal $SiO_2$ quarter-wave layer. A superconducting critical temperature of 8.9 K was extracted from the variation of the resistance with temperature, as illustrated in Fig. 1(a). The surface smoothness was verified by atomic-force microscopy, which showed root-mean square roughness of 0.43 nm, measured in $1 \times 1$ $\mu m^2$ images. The inset of Fig. 1(a) presents an illustration of the surface morphology. The layer thickness was determined precisely using specular hard x-ray reflectivity measurements, depicted in Fig. 1(b), carried out on a PANalytical Empyrean diffractometer. A film thickness of 5.7 nm was extracted from the angular distance between reflection peaks. The experimental curve has been fitted using the GenX software [17]. The geometry of the experimental setup, the cross section of the beam, and the sample size were taking into account for the calculation of geometrical effects near the angle of total external reflection. The fit of the experimental curve shows that the NbN film is rather a bilayer consisting of 3.8 nm of NbN and 1.9 nm of $Nb_xO_y$. This result is consistent with other studies that also showed the presence of the oxide layer on the top of NbN [18]. Such detailed information about the actual composition and thickness of ultrathin superconducting films is mandatory in view of the accurate modelling of the SNSPD performance.

## 3. Results and discussion

The NbN film was patterned into a meander structure by electron-beam lithography and inductively-coupled plasma etching. Figures 2(a) and (b) show scanning electron microscopy (SEM) images of a typical SNSPD meander, with a wire width of 100 nm and a fill factor of 0.5. The diameter of the detector active area is 15 $\mu m$. Prior to further processing, devices were tested under excitation at 1.31 $\mu m$ to assess their polarization sensitivity. The polarization sensitivity of the devices, $C$, is defined as [10]:

$$C = \frac{1 - N_{TM} / N_{TE}}{1 + N_{TM} / N_{TE}}. \tag{1}$$

where $N_{TM}$ and $N_{TE}$ are the device response to TM-polarized light and to TE-polarized light, respectively. At this point, the TM/TE response ratio was $N_{TM}/N_{TE} = 0.56 \pm 0.08$ (average of measurements on 15 devices at a bias current equal to 0.99 times the critical current, $I_b = 0.99I_{crit}$), which means that the polarization sensitivity was $C = 0.28 \pm 0.06$. After this test, a 330-nm-thick $SiN_x$ layer was deposited on the meanders by plasma-enhanced chemical vapor deposition. Then, single devices were isolated and given a keyhole shape using deep reactive ion etching. This shaping allows the insertion of the devices into the fiber sleeve, as illustrated in Fig. 2(c).

To assess the effect of the $SiN_x$ cap layer on the polarization sensitivity, the device performance is modeled using finite-difference time-domain (FDTD) calculations with the commercial *RSoft FullWave* software. The meander is modeled as a single grating period with in-plane boundary periodic conditions, as described in the insets of Figs. 3(a) and (b). Calculations assume a 3.8-nm-thick NbN wire with a width of 100 nm and a pitch of 200 nm. The absorption efficiency is calculated from the difference between the input power and the reflected plus transmitted power, once the steady state is reached. The wavelength dependent

refractive indices were taken from the literature. Their values at 1.55 µm are $5.23 - i5.82$ for NbN [9] and 3.47 for Si. The refractive indices of $SiO_2$ and $SiN_x$ were extracted from ellipsometry measurements. Their values at 1.55 µm are 1.44 for $SiO_2$ and 1.87 for $SiN_x$, respectively.
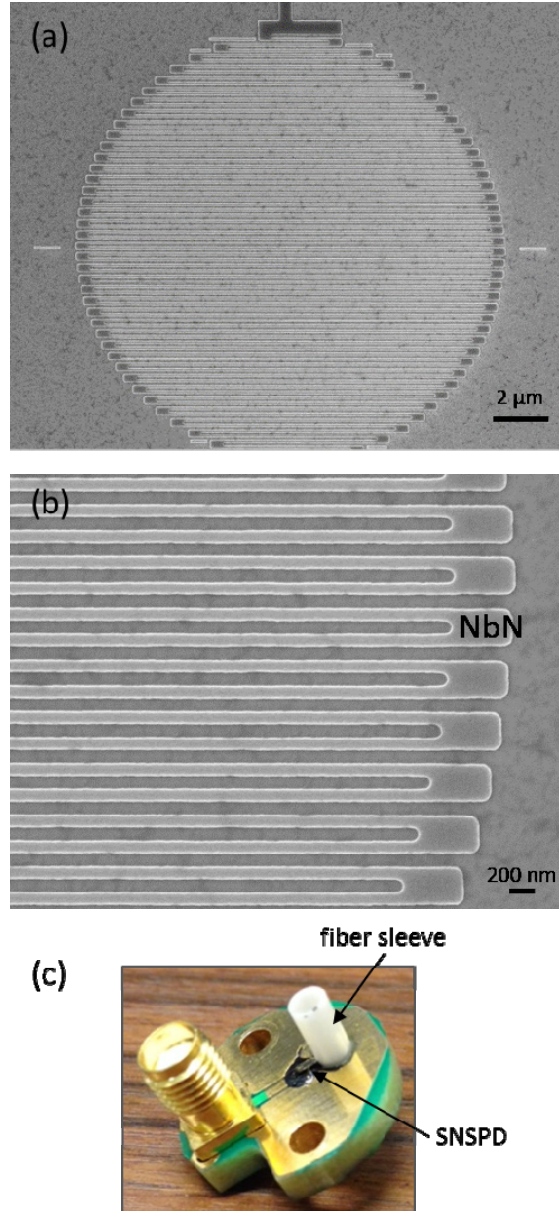


Fig. 2. (a,b) SEM images of the NbN meander. (c) SNSPD device mounted on a print circuit board for characterization.

Figure 3(a) shows the results of calculations performed for a bare NbN wire. The absorption efficiency for TE-polarized light (40.8% at 1.31 µm) is almost twice larger than that for TM-polarized light (22.1% at 1.31 µm), which leads to a polarization sensitivity $C = 0.29$, in good agreement with our experimental result. By depositing a $SiN_x$ cap layer, the TM/TE absorption ratio is increased reaching a value as high as 0.93 at 1.3 µm and 0.85 at

1.55 µm, as illustrated in Fig. 4. The presence of the $SiN_x$ layer generates an additional interference that modulates the response of the detectors both for TE and TM polarization. In the 1.31 to 1.55 µm range, maximum TE response is obtained for a $SiN_x$ layer thickness in the range of 330 to 420 nm, whereas minimum polarization sensitivity (maximum TM/TE ratio) is obtained for a $SiN_x$ thickness in the range of 270 to 350 nm. Therefore, a $SiN_x$ thickness of 330 nm has been chosen as a good compromise to maximize the response and minimize the polarization sensitivity in the 1.31 to 1.55 µm range. The predicted absorption efficiency for a 330 nm $SiN_x$ cap layer is depicted in Fig. 3(b) as a function of wavelength. Note that, in comparison with the uncapped wire, the absorption efficiency of TE-polarized light is only weakly affected by the $SiN_x$ layer (41.4% at 1.31 µm), whereas the absorption efficiency of TM-polarized light is strongly enhanced (36.4% at 1.31 µm). Our model hence predicts $C = 0.064$ and $C = 0.079$ at 1.31 µm and 1.55 µm, respectively.
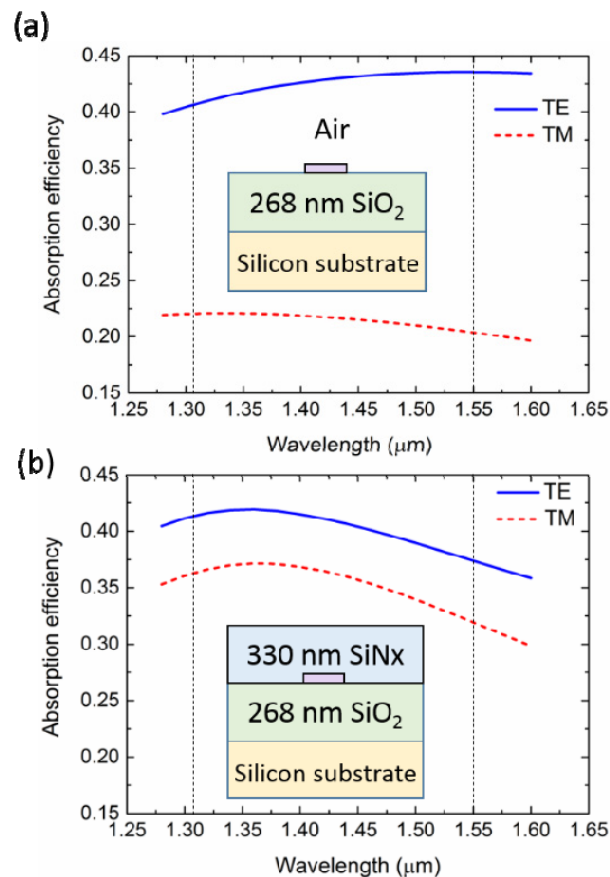


Fig. 3. Calculated absorption efficiency as a function of the wavelength (a) for the uncapped NbN meander; (b) for the NbN meander covered with 330 nm of $SiN_x$. Insets: Designs of the structures for which simulations have been performed.

Note that the values of absorption efficiency in Figs. 3 and 4 are relatively low in comparison with recent experimental results in the literature [6,7]. This is due to our choice of validating the effect of the high-index dielectric cap in the simplest detector geometry, i.e. an NbN meander on a $SiO_2$-on-silicon wafer. Then, the response can be further improved by inserting the nanowire capped with the high-index dielectric layer in a microcavity. For the simplest microcavity geometry, replacing the silicon carrier wafer with a gold mirror,

theoretical calculations predict an absorption efficiency in excess of 90%, while keeping the polarization insensitivity [16].
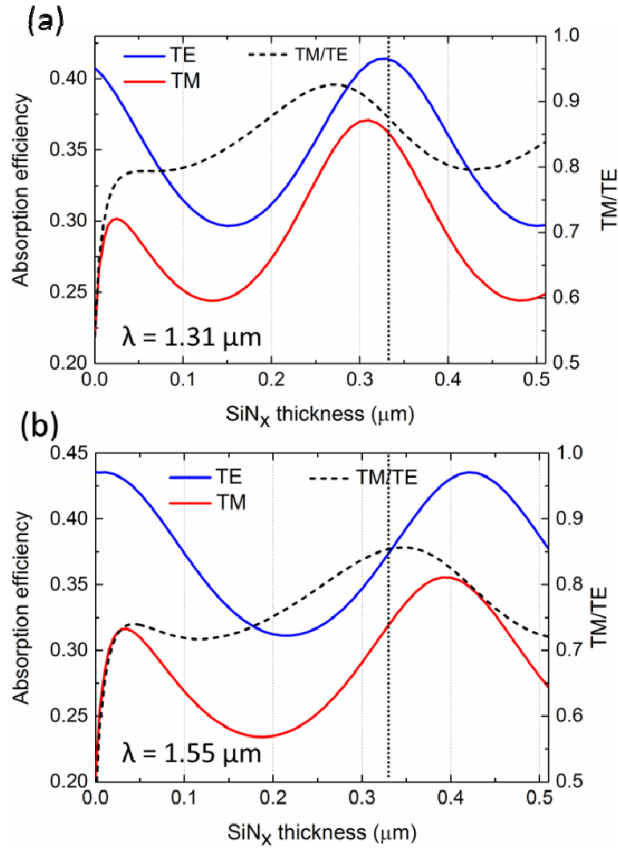


Fig. 4. Calculated dependence of TE and TM absorption efficiency, as well as the TM/TE absorption ratio, as a function of the thickness of the SiN$_x$ cap layer at (a) 1.31 µm, and (b) 1.55 µm.

For characterization of the final detectors, the light from fiber-pigtailed continuous wave laser diodes emitting at 1.31 and 1.55 µm has been coupled into the device from the front side using a self-aligned fiber coupling method which leads to coupling losses below 1% [19]. The laser power was attenuated in order to obtain a photon flux lower than $10^6$ photons/s impinging the device. All measurements were performed at 770 mK. The detection efficiency was calculated by assuming a fiber-detector coupling efficiency equal to 1 and neglecting fiber losses. Figure 5 presents exemplary curves of the detection efficiencies at 1.31 µm and 1.55 µm wavelengths and the dark count rates as a function of the bias current / critical current ratio ($I_b/I_{crit}$). Saturation of the efficiency is reached for $I_b \approx 0.8I_{crit}$ . We measure an $N_{TM} / N_{TE}$ response ratio of 0.86 ± 0.03 and 0.83 ± 0.05 at 1.31 and 1.55 µm, respectively, in agreement with the above-described theoretical predictions (see inset of Fig. 5(b)). This implies polarization sensitivity values of $C = 0.075 ± 0.013$ and $C = 0.093 ± 0.018$ at 1.31 and 1.55 µm, respectively. Deviations from the predicted values (which remain within the error bars) can be assigned to the error in the determination of the refractive indices and layer thicknesses.
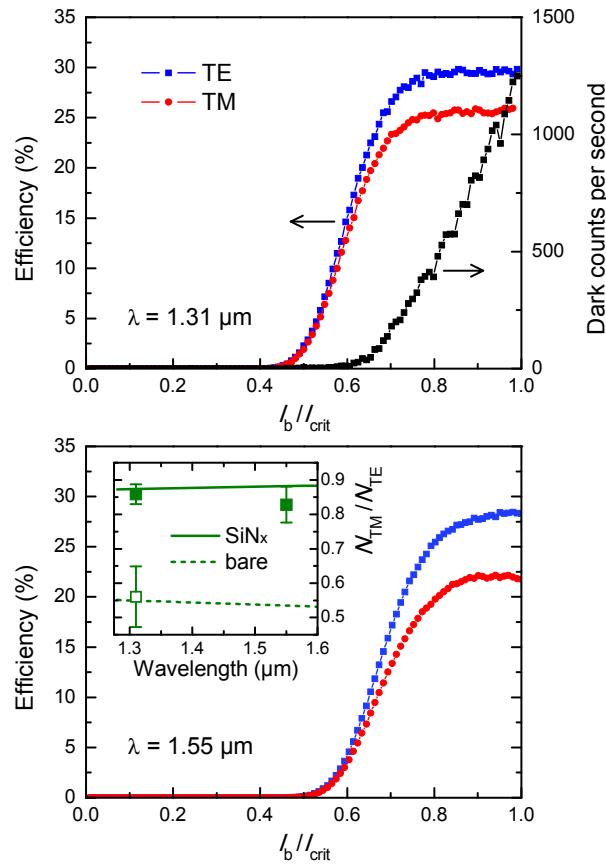
Fig. 5. Detection efficiency as a function of the bias current / critical current ratio ($I_b/I_{crit}$), measured for a typical SNSPD device (a) at 1.31 µm, and (b) at 1.55 µm. The dark count rate is represented in (a). Inset in (b): measurement of the $N_{TM}/N_{TE}$ response ratio of bare devices (open symbol) and devices capped with $SiN_x$ (solid symbols). The curves represent theoretical calculations for both cases.

## 4. Conclusions

In summary, we have fabricated and characterized front-side fiber-coupled SNSPD consisting of an NbN meander on $SiO_2$-on-silicon. We have demonstrated that deposition of a $SiN_x$ dielectric layer on the top of the NbN meander leads to a significant reduction of the polarization sensitivity of the detector, without penalty in terms of detection efficiency. Our experimental results are in good agreement with theoretical predictions, showing that the $SiN_x$ cap layer has no detrimental impact on the internal efficiency. This strategy can be easily combined with more advanced microcavity designs [16] for the fabrication of near-unity efficiency, polarization-insensitive and fiber-coupled SNSPDs.

## Funding